OPENQUATERNARY

Palaeoecological Interpretation of a Late Holocene Sediment Sequence from the Alpine Belt of the Southern Mongolian Altai Mountains

RESEARCH PAPER

SVEN GOENSTER-JORDAN
BRIGITTE URBAN
ANDREAS BUERKERT

*Author affiliations can be found in the back matter of this article

ubiquity press

ABSTRACT

The climate in the Altai Mountains is determined by two major climate systems whose dominance has varied over time, leading to significant spatio-temporal changes in temperature and precipitation during the Holocene. This study aimed at the reconstruction of the local to regional moisture and temperature conditions in an alpine belt of the southern Mongolian Altai during the Late Holocene. It thereby contributes to a more comprehensive understanding of the region's palaeoclimate in the Holocene. Our reconstruction is based on palynological and sediment analyses as well as radiometric age determinations of samples from a 130 cm exposed soil/sediment profile within the alpine belt. Largely supported by sedimentological and geochemical observations, the pollen assemblages indicate a warm and dry period between about 2600 and 2250 cal a BP, a subsequent cold and humid phase extending to about 130 cal a BP, and a return to warm and dry conditions lasting to present. Our data support the results of recent studies on the regional climate variability and the observation of significant differences in the mode of climate changes and its temporal sequence within the Altai Mountains. Although the pollen assemblages in the profile reflected a continuous anthropo-zoogenic influence on the study site's vegetation climatic signals were clearly detectable, underlining the indicator value of the pollen data from the Alpine sediments for regional palaeoclimatic reconstruction.

CORRESPONDING AUTHOR:
Sven Goenster-Jordan
University of Kassel, DE
goenster@uni-kassel.de

KEYWORDS:
^{14}C analysis; A/Cy ratio; Anthropo-zoogenic disturbance; Climate change; Micro charcoal particles; Moisture change; Palaeosol; Pollen analysis; Temperature change

TO CITE THIS ARTICLE:
Goenster-Jordan, S, Urban, B and Buerkert, A. 2022. Palaeoecological Interpretation of a Late Holocene Sediment Sequence from the Alpine Belt of the Southern Mongolian Altai Mountains. *Open Quaternary*, 8: 2, pp. 1–18. DOI: *https://doi.org/10.5334/oq.90*

INTRODUCTION

The climate of the Altai Mountains, which are located in the center of the Eurasian continent, is dominated by westerly winds almost throughout the year (Feng et al. 2017). The westerlies transport warm and humid air masses mainly from Central Asia and the Atlantic Ocean to the Altai Mountains (Aizen et al. 2005; Aizen et al. 2006; Blyakharchuk et al. 2007). This is well reflected in the distribution of precipitation in the Altai Mountains, which is higher on the western side of this range given orographic precipitation and decreases eastward on the leeward side (Feng et al. 2017). Nowadays, about one-tenth of the region's annual precipitation originates from the Pacific Ocean and occurs between spring and autumn (Aizen et al. 2005). During the winter season, the stable Siberian anticyclone transports cold and dry arctic air masses to the Altai Mountains (Klinge et al. 2003; Bezuglova et al. 2012). During the Holocene the precipitation pattern in the Altai Mountains has been subjected to significant spatio-temporal changes (Tarasov et al. 2000; Chen et al. 2008; Feng et al. 2017), due to shifts in the relative power between the North Atlantic system with its westerly airflows, and the Pacific system with its airflows from the east (Feng et al. 2017; Zhang et al. 2018) likely as a result of changes in sea surface temperature in the Atlantic and Pacific Oceans (Sun et al. 2015).

The Altai Mountains are ideal for climate change research not only because of their geographical position, but also given the abundance of potential proxies for climate reconstruction (Schwikowski et al. 2009). The climate variation of this area during the Holocene has been previously reconstructed from numerous proxies such as tree rings (Myglan et al. 2012; Dulamsuren et al. 2014), palaeosols (Fedeneva and Dergacheva 2003), lake levels (Grunert et al. 2000), glacial geomorphology (Schlütz and Lehmkuhl 2007; Blyakharchuk et al. 2008; Agatova et al. 2012; Herren 2013; Ganyushkin et al. 2018), clastic sediment properties (Kalugin et al. 2005), and biological indicators such as diatoms (Westover et al. 2006) and pollen (Rudaya and Li 2013; Huang et al. 2018; Unkelbach et al. 2018). A recent review, based on 30 pollen records, concluded that the climate in the Altai Mountains and the surrounding areas showed a general trend towards cooler and wetter conditions during the Holocene (Zhang and Feng 2018). However, different parts of the mountain range experienced a different climate development in terms of temperature and humidity during the last 11,000 years. Based on Holocene vegetation records Rudaya et al. (2009) suggested that the eastern Mongolian part of the Altai was subjected to a warm and wet climate during the Early Holocene (11,000 to 5000 a BP) and to a cool and dry one during the Late Holocene (5000 a BP to present). In the northern Russian part of the mountain range the Early Holocene was characterized by warm and wet and the Late Holocene by cool and wet climate conditions, while in the western Kazakh Altai the Early Holocene was warm and dry and the Late Holocene cool and wet. Wang and Feng (2013) concluded in a synthesis of pollen records of the Northern Altai Mountains that a relatively warm and wet climate existed between 10,500 and 5000 cal a BP and cool and dry climate prevailed afterwards. Most of the studies included in these meta-analyses focused on the northern part and southern Chinese part of the Altai. In view of uncertainties about the extent and interpretation of climatic and environmental fluctuations, which are subjected to spatial differences within the landscape (Fedeneva and Dergacheva 2003) and to the temporal resolution of proxy data (Rudaya and Li 2013), more information on the southern Mongolian Altai is needed. This contributes to a better understanding of the climate variations in this area during the Late Holocene.

From a palaeoecological perspective, soil profiles have the capacity to integrate a range of environmental variables over time (Targulian et al. 2019). They thus represent a significant terrestrial archive that contains either direct or indirect proxy data through pedogenic properties or fossil pollen extracted from soil horizons, respectively (Fedeneva and Dergacheva 2003; Schlütz and Lehmkuhl 2007). Characteristics of fossil soil pollen assemblages and pollen ratios may allow the reconstruction of palaeovegetation and palaeoclimates (Davidson et al. 1999; Herzschuh 2007; Xu et al. 2007; Li et al. 2010). However, the edaphon and soil physical-chemical processes could lead to differential preservation of pollen grains so that soil pollen data should be interpreted with caution (Xu et al. 2016). Despite these challenges, several studies showed that pollen can be well preserved in mineral soil profiles (Dimbleby 1952; Bałaga and Chodorowski 2006; Buso Junior et al. 2019). Recently, a pollen-climate calibration set from central-western Mongolia was constructed, indicating the response of numerous pollen taxa to variations of temperature and precipitation (Tian et al. 2014) supporting the interpretation of extracted pollen with regard to its palaeoclimatic significance. Furthermore, the ratio of fossil *Artemisia* to Cyperaceae pollen (A/Cy) has been used as a reliable indicator for changes in summer temperature over time in the alpine steppe and alpine meadow (Herzschuh et al. 2006; Herzschuh 2007; Zhao and Herzschuh 2009).

In view of the findings presented above, our study aimed at the reconstruction of the local to regional moisture and temperature conditions in an alpine belt of the southern Mongolian Altai Mountains during the Late Holocene. Thereby, the reconstruction is based

on analyses of palynological and sediment records as well as radiometric age determinations of a sequence of samples from an exposed soil/sediment profile. This study therefore contributes to a more comprehensive understanding of the Holocene palaeoclimate of the Altai Mountains by addressing knowledge gaps for its southern Mongolian part.

MATERIALS AND METHODS

STUDY SITE

The sediment/soil profile is located in the alpine belt of the southern Altai Mountains in the Mongolian Bayan-Ulgii Province (***Figure 1***). From June to August the area surrounding the sediment/soil profile is intensively grazed by livestock of transhumant pastoralists (Jordan et al. 2016). Discharge from surrounding periodic streams into the nearby permanent mountain lake Tsunkhul Nuur occurs following strong precipitation events and during snow melt in spring (***Figure 2a***). About three kilometers southwest of this lake, an intermittent stream flows through a two kilometers wide tributary valley into the Tsunkhul Nuur (***Figure 2b–d***). The stream only flows during May and cuts up to five meters into debris from the valley slopes. Over time this process has resulted in the exposure of the sampled sediment/soil profile (46.633503 N, 91.556486 E, 2583 m a.s.l., ***Figure 2e***).

During 2013 and 2014, the mean annual air temperature in the study area was –3.9°C and –5.2°C, respectively, and annual rainfall amounted to 400 mm and 211 mm, respectively. The long-term records of two nearby weather stations range from –1.4°C to 2.5°C for mean annual air temperature and from 75 mm to 127 mm for annual rainfall amount (Baitag station, 1963–2014, 1186 m a.s.l., ***Figure 1***, southern station; Duchinjil station, 1977–2014, 1951 m a.s.l., ***Figure 1***, northern station.

Cryophyte steppes predominate throughout the area and are typically associated with alpine meadows (Zemmrich 2008; Zemmrich et al. 2010) dominated by the Cyperaceae genus *Kobresia* or at higher elevations by *Carex* (Hilbig 1995). Characteristic elements of the alpine steppe are *Dracocephalum bungeanum* Schischk. & Serg., *Cirsium esculentum* (Siev.) C.A. Mey., *Saussurea pseudoalpina* N.D. Simpson, *Scorzonera austriaca* Willd., Fabaceae such as *Trifolium eximium* DC. and species of *Artemisia*. Among the shrubs, *Ephedra przewalskii* Stapf grows on open and dry stands such as along slopes, while *Ephedra monosperma* J.G. Gmel. ex C.A. Mey. occurs at various habitats in the upper mountain steppes. *Ephedra equisetina* Bunge is frequently found in stony areas of the alpine steppe. Besides Cyperaceae (mainly *Carex melanantha* C.A. Mey., *C. duriuscula* C.A. Mey., *C. melanocephala* Turcz.), the alpine meadow

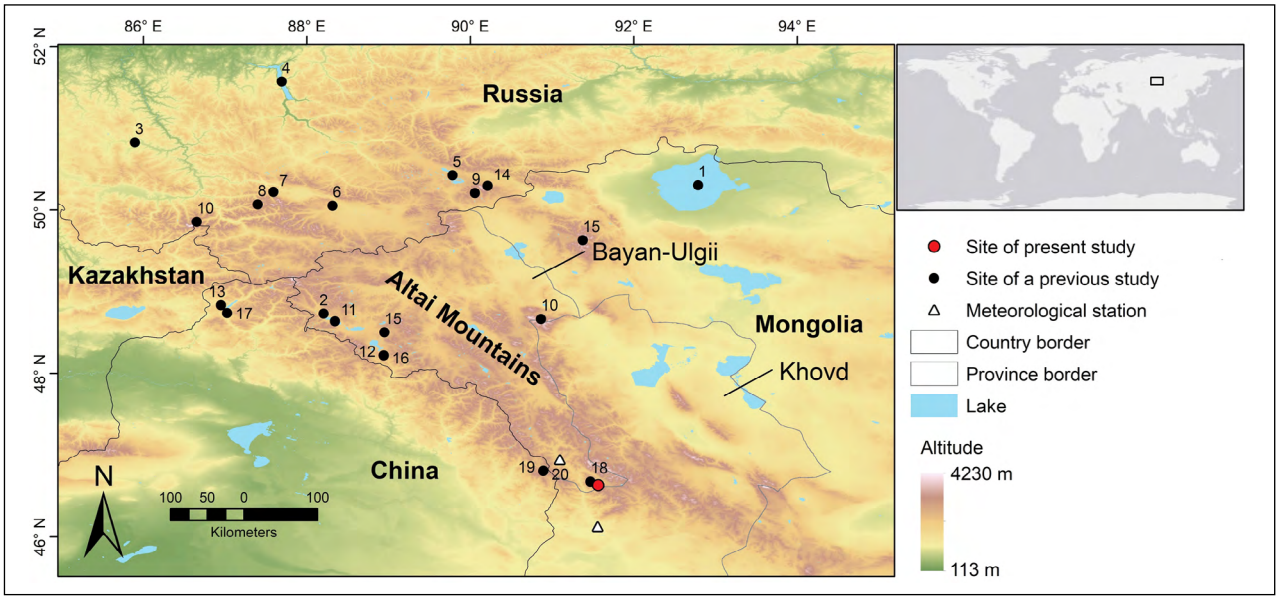

Figure 1 Locations of the present study and the meteorological stations of Duchinjil (northern) and Baitag (southern) in the southern Mongolian Altai Mountains. Additionally, the locations of other studies on the reconstruction of the environmental/climatic conditions in this mountain range during the Holocene are presented. Site 1: Uvs Nuur Basin (Grunert et al. 2000); site 2: Hoton Nuur Basin (Tarasov et al. 2000); site 3: Central Russian Altai (Fedeneva and Dergacheva 2003); site 4: Lake Teletskoye (Kalugin et al. 2005); site 5: Kurai and Karaginskaya Basin (Westover et al. 2006); site 6: Kuray and Chuya Basin (Schlütz and Lehmkuhl 2007); site 7: Dzhangyskol Lake (Blyakharchuk et al. 2008); site 8: North Chuya Range (Agatova et al. 2012); site 9: Mongun Taiga Mountain Massif (Myglan et al. 2012); site 10: Belukha and Tsambagarav Mountains (Herren 2013); site 11: Hoton Nuur (Rudaya and Li 2013); site 12: mountain range near Dayan Nuur (Dulamsuren et al. 2014); site 13: Kanas Lake Basin (Feng et al. 2017); site 14: Mongun-Taiga Massif (Ganyushkin et al. 2018); site 15: Kharkhiraa and Tsengel Mountains (Klinge et al. 2017); site 16: mountain range near Dayan Nuur (Unkelbach et al. 2018); site 17: Kanas Lake (Huang et al. 2018); site 18: southern Altai (Oyunmunkh et al. 2019); site 19 and 20: Yushenkule Peat (Yang et al. 2019a; Yang et al. 2019b).

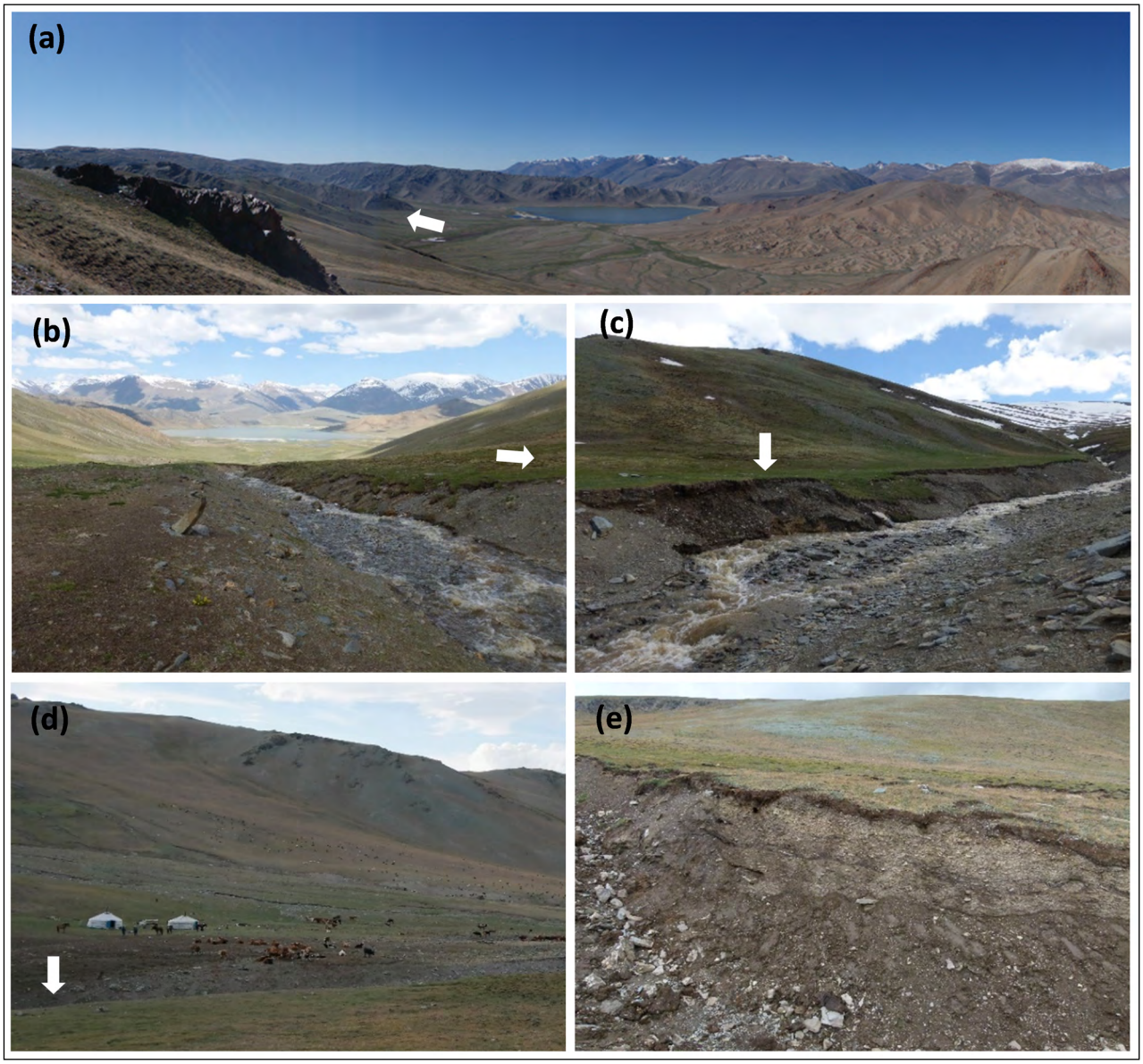

Figure 2 Images of the study site; photo **(a)** provides an overview of the summer pasture at Tsunkhul Lake, Mongolian Bayan-Ulgii Province, the arrow indicates the entrance of the valley with the soil/sediment profile; photo **(b)** provides a view down the valley towards Tsunkhul Lake, the profile is located about 20 meters to the right of the arrow; photo **(c)** provides a view up the valley, the arrow indicates the location of the soil/sediment profile; photo **(d)** illustrates the pasture utilization by livestock in the surrounding of the soil/sediment profile, the location of the profile is indicated by the arrow; photo **(e)** shows the exposed soil/sediment profile.

is characterized by Poaceae (*Festuca altaica* Trin. ex Ledeb., *Poa attenuata* Trin., *Poa* spp., *Hordeum brevisubulatum* (Trin.) Link) accompanied by a rich herbal flora consisting of Asteraceae (e.g. *Taraxacum*), Chenopodiaceae (subfamily of the Amaranthaceae; e.g. *Eurotia ceratoides* (L.) C.A. Mey. and *Chenopodium album* L.), *Suaeda przewalskii* Bunge, *Potentilla* spp., *Androsace chamaejasme* Wulfen, *Primula farinosa* L. and *Glaux maritima* L. The nearest woodland is located about 4.5 km southwest of the profile. It consists exclusively of *Larix sibirica* Ledeb. on the northern slopes at an altitude of about 2600 m a.s.l.

SAMPLING STRATEGY AND ANALYSES

The profile showed a clearly distinguishable alternating sequence of dark and light colored layers down to a depth of 170 cm (***Figure 2e*** and ***3***). In summer 2013, a sample was taken from each of 10 identified dark colored layers (labeled with an A; assumed to have high levels of organic carbon) and each of the 10 identified light colored layers (labeled with a B; assumed to have low levels of organic carbon) along a vertical line. Because of the large thickness, two samples were taken from the deepest light colored layer. Each sample represented mixed material, which was collected between the upper and lower boundary of each layer. A large charcoal piece, found at a depth of 106 cm, and bone fragments, found at 102 cm and 113 cm, were additionally sampled and stored in separate polypropylene bags. All layer samples were air-dried, sieved to <2 mm and then subjected to chemical analysis and, additionally in the case of the dark colored layers, ^{14}C dating and pollen preparation.

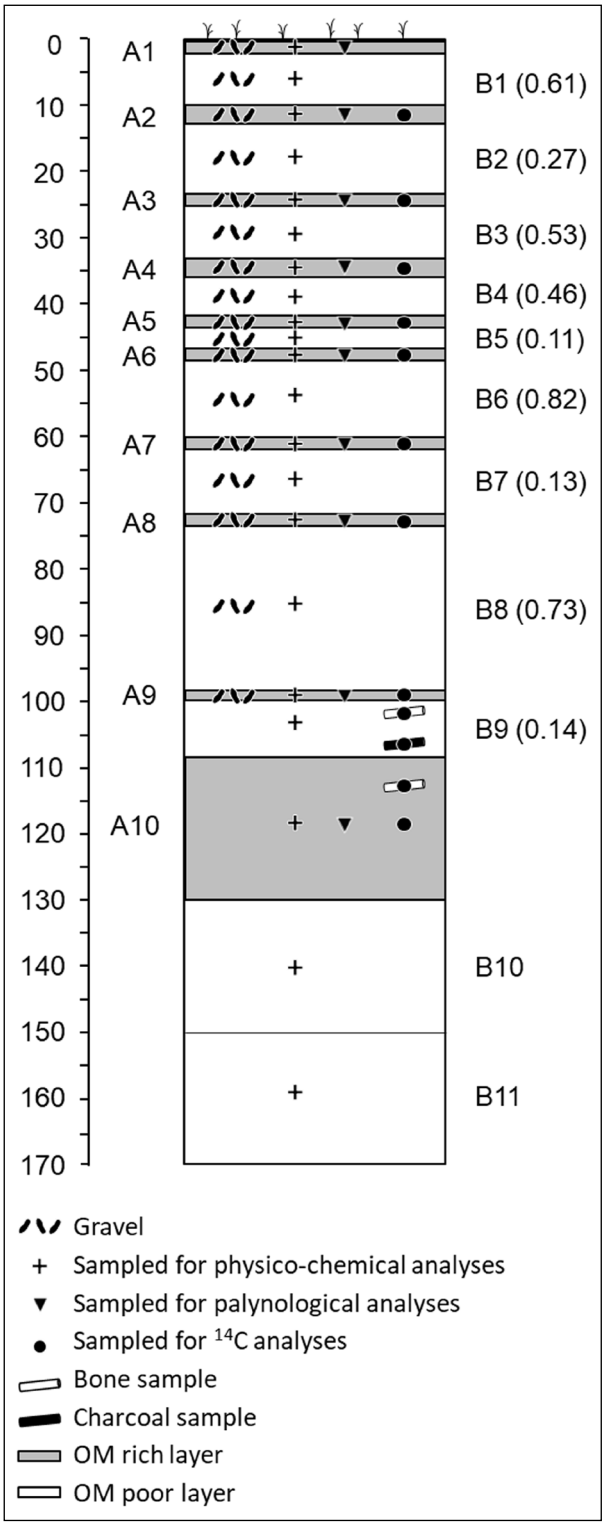

Figure 3 Sketch of the sampled soil/sediment profile at Tsunkhul Lake in the southern Mongolian Altai Mountains. Depth of upper and lower boundaries of organic matter (OM) enriched layers (labeled with A) and OM poor layers (labeled with B) are shown. Additionally, sampling depths of bone and charcoal samples, ^{14}C and palynological samples, and soil samples for physico-chemical analyses are provided. Depth indications are given in cm. Numbers in brackets indicate the sedimentation rate of the B layers in mm per year.

After addition of 10% HCl, the concentration of $CaCO_3$ was measured gas-volumetrically using a calcimeter (Calcimeter Bernard, Prolabo, Paris, France) according to Blume et al. (2011). For the analyses of total carbon (C_{total}) and total nitrogen (N_{total}), samples were oven dried (60°C, 24 h) and subsequently ground with a ball mill. Concentration of organic carbon ($C_{organic}$) was determined indirectly by calculating the difference between $CaCO_3$-C and C_{total}. Concentrations of N_{total} in the samples were determined by an element analyzer (vario Max CN Element Analyzer, Elementar Analysesysteme GmbH, Hanau, Germany). Air-dried layer samples were used for the measurement of available PO_4-P (P_{Bray-2}). Following the extraction with 0.1 N HCL and 0.03 N NH_4F, concentrations of P_{Bray-2} were measured colorimetrically with a spectrophotometer (Hitachi U-2000, Hitachi Ltd., Tokyo, Japan) at a wavelength of 882 nm (Bray and Kurtz 1945).

DATING OF SAMPLES

Following standard procedures of dating labs, ^{14}C dating of the dark colored layers, bones and a charcoal piece was carried out at the Poznan Radiocarbon Laboratory (Poznan, Poland) using an accelerator mass spectrometer (AMS; 1.5SDH Pelletron Model Compact Carbon AMS, National Electrostatics Corp. NEC, Middleton, WI, USA). After removing roots and organic acids by treatments with HCl and NaOH, collagen of bone samples was used for dating as sufficient N was found in the samples (≥0.7%) and the C/N ratio was ≤1%. The radiocarbon ages (age ^{14}C a BP) were calibrated against the IntCal 20 calibration data set (Reimer et al. 2020) with the online version of the Oxcal program (version 4.4, Research Laboratory for Archaeology and the History of Art, University of Oxford, UK). The results were presented as calibrated age in years before present (age cal a BP) whereby 'present' is defined as AD 1950. To model the age of non-measured depths, a quadratic polynomial regression was fitted to the data set of age cal a BP using SigmaPlot 12.0 (Systat Software Inc., San José, CA, USA). Based on the thickness of the B-layers and the dating of the overlying and underlying A-horizons, the sedimentation rate was calculated. The rates provide valuable information on the sedimentation intensity over the corresponding period.

PALYNOLOGICAL ANALYSES

Nine samples of the layers assumed to be rich in OM (all A layers except for A5 due to a lack of sufficient sample material) were transferred to the laboratory of the Institute of Ecology at Leuphana University of Lüneburg (Germany) for palynological analysis. For this purpose, sub-samples of 10 to 20 g were treated by standard palynological methods. These consisted of a carbonate-removal pre-treatment with hydrochloric acid, dispersion with 10% NaOH, flotation to separate organics from the inorganic matrix using sodium metatungstate ($3Na_2WO_4\ 5WO_2\ H_2O$) and acetolysis (Fægri et al. 1989; Moore et al. 1991). The prepared residues were embedded

in glycerine on microscope slides. Due to the relative small amount of available sampling material, only one slide of 24 × 32 mm per sample could be analyzed for pollen and non-pollen palynomorphs with a transmission light microscope using a 400× magnification. Pollen and spores were identified using the atlases of Fægri et al. (1989), Moore et al. (1991) and Beug (2004), and a reference collection at the laboratory of the Institute of Ecology at Leuphana University of Lüneburg, Germany. Micro-charcoal particles with a size of >10 µm and <100 µm were semiquantitatively assessed in the slides by scanning a quarter of the microscopic image section at 100× magnification.

The total pollen sum, on which percentages of all recorded pollen and non-pollen palynomorphs are based, was obtained from terrestrial taxa including Cyperaceae. To ensure a sound interpretation of data, statistical analysis was carried out only on those samples achieving a basic sum >100 (Brugger et al. 2018). Pollen calculations for diagram construction (***Figure 6***) were performed with the software packages TILIA, TILIA GRAPH and TILIA VIEW (Grimm 1990). The first column of the pollen diagram shows the ratio between non arboreal pollen (NAP), which represents the sum of terrestrial herbs, and the arboreal pollen (AP), which is mainly composed by *Ephedra* pollen, but includes long distance transported *Larix* and cf. *Juniperus* pollen. Pollen of *Ephedra* species were categorized either into the *Ephedra fragilis* type s.l. (Ef) or the *Ephedra distachya* type (Ed) (Welten 1957; Lang 1994). Species of the Ef pollen type have been attributed to desert vegetation whereas those of the Ed pollen type are known to be particularly sensitive to semi-desert or steppe climates (Tarasov et al. 1998; Herzschuh et al. 2004). Some pollen grains, which were difficult to determine to genus or species level are indicated at a higher taxonomic level such as e.g. Rubiaceae (cf. *Galium*) or Chenopodiaceae indeterminate in the pollen diagram. For Chenopodiaceae, recent vegetation mapping at and around the sediment/soil profile revealed *Eurotia ceratoides* and *Chenopodium album* (Chuluunkhuyag, 2015, unpublished) suggesting that most of the pollen deposited in the profile likely derive from those species. The herbal taxa presented in the main pollen diagram were assigned to three major categories (alpine steppe, alpine meadow, and forest) representing their preferential ecological distribution. Herbal pollen that could not be determined due to taxonomical reasons were classified as '*varia*', whereas palynomorphs deriving from the geological parent material of the soil or sediment were classified as 'reworked'.

For sound assessment of the palaeoclimate, only pollen taxa with a relatively high percentage within the pollen spectrum and a distinct response to changes in temperature and precipitation were interpreted. A recently published local calibration data set was used to evaluate the response of individual taxa to climatic changes (Tian et al. 2014). The focus was additionally on pollen and spore taxa, which indicate an anthropo-zoogenic influence on the vegetation, possibly leading to a bias in palaeoclimatic interpretation (Li et al. 2015). Less frequent pollen taxa were only interpreted if they could clearly be assigned to the alpine steppe or alpine meadow, and if they therefore could contribute to the evaluation of the precipitation conditions which distinguish the two grassland types. Based on the pollen counts, the ratio of *Artemisia* to Cyperaceae pollen (A/Cy) was calculated as it was considered a reliable indicator for changes in summer temperature over time particularly in the alpine steppe and alpine meadow (Herzschuh et al. 2006; Herzschuh 2007; Zhao and Herzschuh 2009).

RESULTS

DATING OF SAMPLES AND PROPERTIES OF THE PROFILE

The means of the ^{14}C dated samples of dark colored layers, bones and charcoal range from 131 ± 77 to 5643 ± 35 cal a BP (***Table 1***). With the exception of the bone fragments at 113 cm depth, the age cal a BP increases consistently with soil depth and can be well described by a quadratic polynomial regression model (R^2_{adj} = 0.98; ***Figure 4***). The bone samples were identified as the remains of a musk deer (*Moschus* sp.; Prof. Dr. Norbert Benecke, German Archaeological Institute (DAI), Berlin, personal communication).

The alternating series of dark and light colored layers of the profile corresponds to an alternating sequence of concentrations of $C_{organic}$ and N_{total}. Thereby, the dark colored layers show a higher concentration of these parameters compared to the adjacent light colored layers, indicating that the color brightness of the layer is associated with the OM content (***Figure 5***). The average concentration of $C_{organic}$ and N_{total} in the profile is 4.0% and 0.4%, respectively. Highest concentrations of $C_{organic}$ and N_{total} are measured in the layers A1 (7.9%) and A9 (0.8%). P_{Bray-2} values are lower in almost all dark colored layers than in the adjacent light colored ones. Concentrations of P_{Bray-2} vary around 61 µg g^{-1} along the profile, while values of more than 100 µg g^{-1} are measured in layers B1, B8, and B9.

Regarding the profile structure, it was observed that a 10 cm thick layer containing no gravel (layer B9) overlaid a pronounced organic layer with a total thickness of 21 cm (layer A10). The overlaying segment of the profile consists of an alternating sequence of thin layers rich in OM (0.5 cm to 3 cm) and layers with varying thickness (2 cm to 25 cm) containing substantial amounts of non-rounded gravel. A striking feature is the strong variation of sedimentation rates along the profile ranging from 0.11 to 0.82 mm a^{-1} (***Figure 3***). Highest rates are observed for the layers B1, B3, B6, and B8 with values of 0.61, 0.53,

LABORATORY CODE	LAYER		MATERIAL	AGE ^{14}C A BP		AGE CAL A BP			
	DEPTH	ID				FROM	TO	MEAN	
Poz-62376	11.5	A2	Organic matter	35	±30	256	33	131	±77
Poz-58598	24.5	A3	Organic matter	510	±30	623	501	533	±22
Poz-62373	35.0	A4	Organic matter	790	±30	736	670	704	±19
Poz-58599	43.5	A5	Organic matter	965	±30	927	792	857	±41
Poz-62374	48.5	A6	Organic matter	1265	±30	1285	1079	1210	±48
Poz-58600	60.5	A7	Organic matter	1465	±30	1389	1302	1344	±24
Poz-62375	73.5	A8	Organic matter	2265	±30	2345	2156	2254	±61
Poz-58602	99.3	A9	Organic matter	2505	±30	2729	2489	2596	±74
Poz-69381	102.0	–	Bones	3060	±30	3361	3176	3275	±49
Poz-57174	106.0	–	Charcoal	3120	±35	3443	3232	3328	±52
Poz-69382	113.0	–	Bones	2965	±35	3315	2999	3129	±63
Poz-68793	119.5	A10	Organic matter	4920	±30	5718	5591	5643	±35

Table 1 AMS ^{14}C dating of organic matter, bones and charcoal sampled from the soil/sediment profile layers at Tsunkhul Lake in the southern Mongolian Altai Mountains. Depth in cm represents the midpoint of the sampled layers. ^{14}C ages and mean values of calibrated ages before present (cal a BP, whereas 'present' is defined as AD 1950) are presented ± one standard deviation. Dates were calibrated with Oxcal 4.4 using the IntCal 20 calibration curve. The range of calibrated ages represents a 95.4% probability.

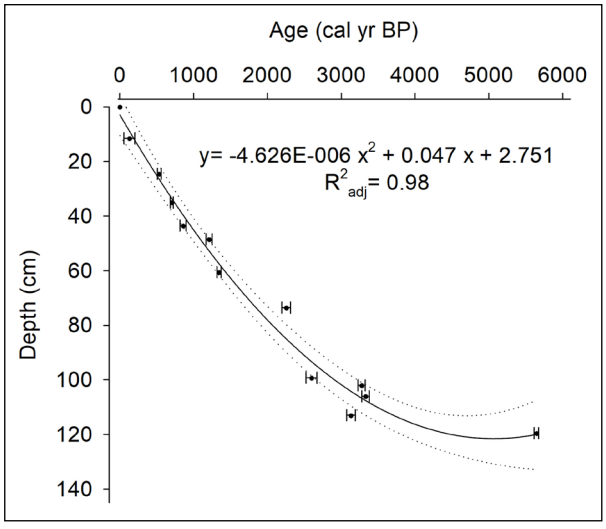

Figure 4 Depth/age model for the soil/sediment profile at Tsunkhul Lake in the southern Mongolian Altai Mountains. Age is given in mean calibrated years before present (cal a BP, while 'present' is defined as AD 1950). Dates were calibrated with Oxcal 4.4 using the IntCal 20 calibration curve. Error bars show ± one standard deviation. Dotted lines represent the 95% confidence interval.

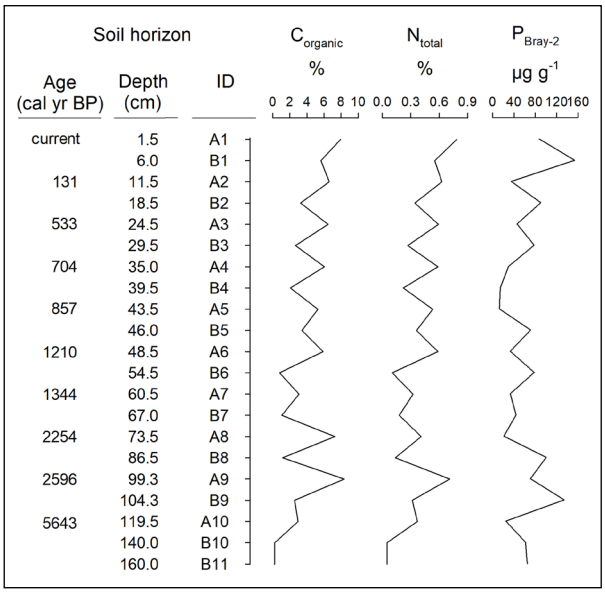

Figure 5 Physico-chemical properties of soil/sediment profile layers at Tsunkhul Lake in the southern Mongolian Altai Mountains. The calibrated ages before present (cal a BP, where 'present' is defined as AD 1950) represent the mean age of organic layers. Depth data represent the average of the upper and lower boundary of each layer. Organic matter enriched layers analyzed for pollen and non-pollen palynomorphs are labeled with an 'A', organic matter poor layers with a 'B'.

0.82, and 0.73 mm a^{-1}, respectively, while the other B layers show rates <0.46 mm a^{-1}.

PALYNOLOGICAL ANALYSES

The total sum of pollen and non-pollen palynomorphs layers rich in the OM ranges between 15 (A10) and 544 (A6) counts, resulting in non-consideration of A10 due to a low pollen sum and the associated uncertainties in the interpretation (***Figure 6***). During the palynological description of the layers the focus is set on pollen of Ed, Cyperaceae and Chenopodiaceae as these pollen taxa occur in all layers, are relatively abundant, and allow a distinct assessment of temperature and/or moisture conditions according to Tian et al. (2014). Additionally,

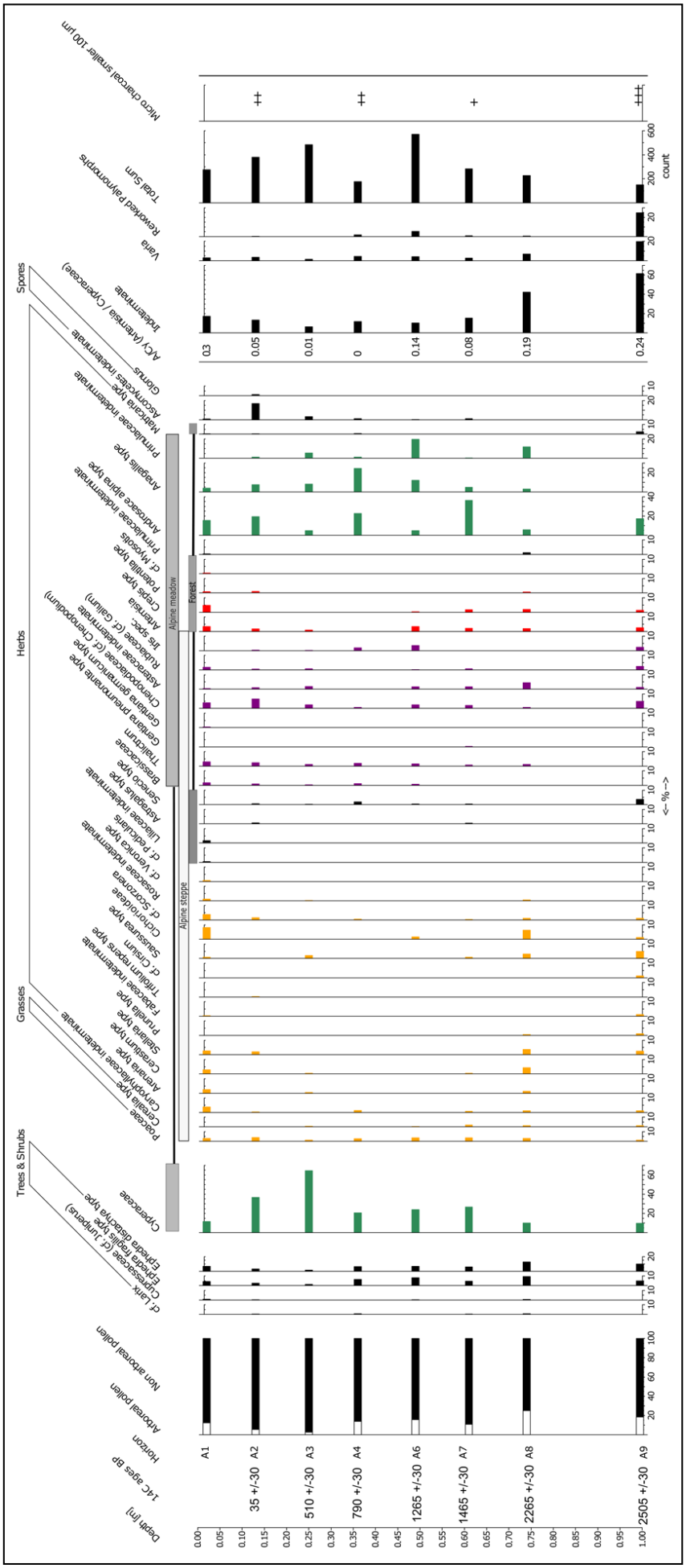

Figure 6 Pollen diagram of the soil/sediment profile at Tsunkhul Lake in the southern Mongolian Altai Mountains. Abundance values are given in percent of the total pollen sum. The ratio of *Artemisia* to Cyperaceae pollen (A/Cy) was calculated based on the pollen counts. Herbal taxa were assigned to their preferential ecological distribution (alpine steppe, alpine meadow, and forest). Micro-charcoal categories: + = rare, ++ = frequent, +++ = highly abundant.

Artemisia pollen is considered more closely, which is also observed in almost all layers and necessary for the calculation of the A/Cy ratio. This pollen taxon is also highlighted due to its indicator potential of possible anthropo-zoogenic impact (Li et al. 2015) in addition to pollen of Asteraceae (Li et al. 2015), *Iris* spec. (cf. lacteal; Baranova et al. 2016), Rubiaceae (cf. *Galium*) and Caryophyllaceae (Li et al. 2008). For the description of moisture-induced shifts of the vegetation between the alpine steppe and the alpine meadow, pollen taxa are included which do not have high indicator qualities (e.g. *Androsace alpina* type (cf. *Androsace chamaejasme*) or *Anagallis* type (cf. *Glaux maritima*)) and partly no high abundance (e.g. Cichorioideae indeterminate, cf. *Scorzonera, Saussurea* type), but can be clearly assigned to the alpine steppe or alpine meadow.

LAYER A9 (99.5–99 CM, 2596 ± 74 CAL A BP)

This layer shows the lowest number of pollen (about 175) including the largest amount of indeterminate (62), of *varia* (20), and of reworked pollen (25). Similar to layer A1 and A8, layer A9 shows the lowest percentage of Cyperaceae pollen (10%) in the profile and a high assignment of pollen to alpine steppe elements (≥10) such as *Stellaria* type (cf. *Stellaria dichotoma* L., 3%) and *Saussurea* (5%). For the latter the highest value within the profile is observed, as well as for Rubiaceae (3%). Pollen of *Iris* spec. show relatively high values of about 3%. The Ed type pollen accounts for 10% most likely from *Ephedra monosperma* and *Ephedra equisetina*, which are currently abundant around the profile. The proportions of Chenopodiaceae and *Artemisia* pollen account for 5% and 3%, respectively. The A/Cy ratio is relatively high (0.24) compared to the upper A-layers and shows the second highest value after layer 1 (***Table 2***). The maximum value of micro-charcoal is also observed in layer A9.

SAMPLE	DEPTH	AGE	A/CY
	CM	CAL A BP[a]	RATIO
A1	1.5	current	0.30
A2	11.5	131	0.05
A3	24.5	533	0.01
A4	35.0	704	0[b]
A6	48.5	1210	0.14
A7	60.5	1344	0.08
A8	73.5	2254	0.19
A9	99.3	2596	0.24

Table 2 *Artemisia*/Cyperaceae (A/Cy) pollen ratio across the soil/sediment profile at Tsunkhul Lake in the southern Mongolian Altai Mountains. Depth represents the midpoint of the sampled layer. The calibrated age before present (cal a BP, whereas 'present' is defined as AD 1950) represents the mean age of the layer.

[a]Dates calibrated with Oxcal 4.4 using the IntCal 20 calibration curve; [b]A lacking, Cy 24%.

LAYER A8 (74–73, 2254 ± 61 CAL A BP)

In addition to the same low percentages of Cyperaceae pollen (about 10%), layer 8 shows a similar diverse occurrence of herbal alpine steppe elements as layer A9, though different taxa are dominant. Besides the pollen taxon Caryophyllaceae indeterminate, *Arenaria* type and *Saussurea* type, which each account for less than 3%, the steppe elements mainly comprise *Cerastium* type (cf. *Cerastium arvense* L., 4%), *Stellaria* type (4%) and Cichorioideae indeterminate (7%). Ed type pollen is with 12% highest in the entire profile. While the proportion of Chenopodiaceae pollen is insignificant (<1%), *Artemisia* pollen accounts for about 2%. The A/Cy ratio is with 0.19 relatively low.

LAYER A7 (61–60 CM, 1344 ± 24 CAL A BP)

While the proportion of Cyperaceae pollen increases to 26%, layer A7 shows a lower number of pollen taxa that can be clearly assigned to the herbal alpine steppe compared to A8 and A9. Only Caryophyllaceae indeterminate, *Cerastium* type, *Saussurea* type and cf. *Scorzonera* occur with rather low values (<2%). *Artemisia* and Chenopodiaceae indeterminate are present with low values of about 2%. However, pollen of *Androsace alpina* type shows the highest value (37%) of the profile. The Ed type pollen proportion of the total pollen amount is 5.5%. The A/Cy ratio (0.08) is smaller compared to A8. Only a few micro-charcoal particles are observed in this layer.

LAYER A6 (49–48 CM, 1210 ± 48 CAL A BP)

Like layer A7, the pollen spectrum reveals a dominance of taxa that can be clearly assigned to an alpine meadow. Cyperaceae pollen accounts for 24%, while pollen of *Artemisia, Iris* spec. and *Primula farinose* type record with 3.5%, 4% and 19%, respectively, highest values within the profile. For the category of alpine steppe herbs, only a weak signal of Cichorioideae indeterminate pollen (2%) is observed. Pollen of Ed type accounts for 8%. The ratio of A/Cy (0.14) is slightly higher than the one of layer A7 but still on a low level.

LAYER A4 (36–34 CM, 704 ± 19 CAL A BP)

The pollen spectrum of layer A4 has a similar percentage of Cyperaceae pollen as layer A6. Remarkable are the high amounts of the meadow pollen taxa *Androsace alpina* type and of *Anagallis* type (both 25%), the latter displaying its maximum value within the profile. In contrast, pollen of alpine steppe herbs are rarely observed, in fact only Caryophyllaceae indeterminate and cf. *Scorzonera* are recorded with low percentages (<2%). Pollen of *Iris* spec. shows relatively high values of about 2%. *Artemisia* pollen is lacking, leading arithmetically to an A/Cy ratio of 0. Pollen of the Ed type accounts for 7% of the layer's total pollen sum. Micro-charcoal is frequently observed.

LAYER A3 (25–24 CM, 533 ± 22 CAL A BP)

Similar to the three underlying layers A4, A6 and A7, pollen of the alpine meadow elements dominates while signals of alpine steppe herbs are rather low. Layer A3 reveals for example the highest pollen percentages for Cyperaceae (65.5%) of the entire profile, whereas only pollen of the *Saussurea* type (2%) is found in significant amounts in the category of alpine steppe herbs. Furthermore, high percentages of spores of Ascomycetes indeterminate (5%) and very low amounts of Artemisia pollen (1%) are noted. Ed type pollen has the lowest value within the profile and accounts for less than 2% of the total pollen amount in the layer. The ratio of A/Cy (0.01) is rather low.

LAYER A2 (13–10 CM, 131 ± 77 CAL A BP)

Layer A2 is also characterized by a high proportion of Cyperaceae pollen (27.5%), leading again together with relatively high percentages of *Androsace alpina* type (20%) and *Anagallis* type pollen (8%) to a dominance of the alpine meadow elements in the pollen spectra. For the alpine steppe herbs, only *Stellaria* type and cf. *Scorzonera* pollen are observed in significant amounts (each 2%). In contrast, the highest percentages for pollen of Chenopodiaceae indeterminate (6%) and spores of Ascomycetes indeterminate (13%) are recorded in this layer. Noteworthy is the occurrence of spores of *Glomus* type (2%), which is only observed in A2. Pollen of *Artemisia* accounts for 1.5% and the ratio of A/Cy is rather low (0.05). Pollen percentage of the Ed type has the second lowest value across the profile (5%). Micro-charcoal particles are frequently observed.

LAYER A1 (2–0 CM, PRESENT)

The pollen spectrum of the recent layer A1 shows a higher diversity of herbaceous taxa and a more balanced proportion of steppe and meadow elements than the five A-layers (A2 to A7) below. While pollen percentages of Cyperaceae (11%), *Androsace alpina* type (16%) and *Anagallis* type (5%) are relatively low, herbs of the alpine steppe are rather frequent, whereas pollen of Caryophyllaceae indeterminate, *Arenaria* type, *Cerastium* type, *Stellaria* type, Cichorioideae indeterminate and *Scorzonera* dominate with values between 3 and 8%. The maximum value for *Artemisia* pollen is recorded in this layer (4%) resulting in the highest A/Cy ratio (0.30) of the profile. Pollen percentages of the Ed type accounts for 8% of the total pollen amount in this layer.

DISCUSSION

LATE HOLOCENE VARIATIONS IN CLIMATE

The pollen type Ed, Cyperaceae and Chenopodiaceae are selected for interpretation of the palaeoclimate not only due to their relatively high percentages across the profile, but also because of their indicative value in terms of precipitation and temperature changes for central-western Mongolia (Tian et al. 2014). The latter is based on their steady and relatively strong increase or decline in response to climate change. While the amount of Cyperaceae pollen declines with decreasing precipitation, Ed type pollen shows an increasing trend, particularly under very arid conditions (about <150 mm a^{-1}; Tian et al. 2014). It is generally assumed that the amount of Chenopodiaceae pollen increases with rising aridity (Ma et al. 2020), but a strong decline of this pollen type can be observed under very arid conditions in central-western Mongolian regions (Tian et al. 2014), hampering a distinct climate interpretation under arid conditions. However, the proportion of Chenopodiaceae pollen steadily increases with rising average temperatures in July, as is the case with pollen of the Ed type, particularly under very warm conditions (about >18°C; Tian et al. 2014). For the central Tibetan Plateau, A/Cy ratio values <1 indicate an alpine steppe vegetation (Herzschuh et al. 2006), while it can be observed that very small values (<0.1) correspond to an alpine meadow (Kürschner et al. 2005). This ability of the ratio to differentiate an alpine steppe from an alpine meadow points to its significant correlation with the annual precipitation (negative) and the average temperature in July (positive) (Herzschuh 2007).

The A/Cy ratio can generally be considered as low with values ≤0.30 (Yu et al. 2008; Herzschuh et al. 2006), which indicates a cold alpine environment during the last 2600 years. This is confirmed by a pollen taxa composition of an alpine meadow and alpine steppe. Due to the continuous and relatively high abundance of *Ephedra*, *Artemisia* and Chenopodiaceae pollen across the layers of the profile, a rather dry climate can be assumed for the observed period. Although the vegetation is not subjected to major changes as indicated by the pollen spectra, observed minor changes in its composition may suggest slight climate variations in the surroundings of the site during the Late Holocene that can be divided into three stages. The pollen data suggest that a relatively warm and dry climate prevailed in 2596 and 2254 cal a BP, indicated by high percentages of the Ed type pollen, low proportion of Cyperaceae pollen, and a relatively high A/Cy ratio. Additionally, a comparatively high diversity of the herb steppe taxa can be observed with partly relatively high percentages, in contrast to the pollen of the alpine meadow herbs showing lower amounts. It can be assumed that the climate in 2254 cal a BP could have been even drier than in 2596 cal a BP, which is indicated not only by the more pronounced occurrence of steppe taxa and the maximum of Ed type pollen, but also by the very low percentage of Chenopodiaceae pollen. For the time span between 1344 and 131 cal a BP pollen assemblages indicate a rather cold and wet climate. Cyperaceae pollen percentages are relatively high, while Ed type pollen as well as the A/Cy show low values. Low

Chenopodiaceae pollen percentages additionally point to a rather cold environment, whereas the maximum in 131 cal a BP appears to contradict this assumption. However, the maximum of Ascomycetes indeterminate spores likely indicates a high anthropo-zoogenic influence amplifying the pollen signal of the nitrophilious Chenopodiaceae (Li et al. 2008; Gunin et al. 1999). The maximum of this colder and wetter period can be observed at 533 cal a BP coinciding with the minimum of Ed type pollen, the maximum of Cyperaceae, and a very low A/Cy ratio. The recent pollen assemblage of layer A1 reveals again a return to relatively warm and dry climatic conditions. The assumption of rather dry climatic conditions is suggested by the low amounts of Cyperaceae, which are comparable to those of layer 8 and 9, and the relatively high proportion of Ed type pollen, which, however, is not reaching the values of the two layers mentioned. The very high value of the A/Cy ratio and of Chenopodiaceae points to a relatively warm climate. Additionally, the general abundance and rather diverse composition of herbal alpine steppe taxa in combination with relatively low percentages of alpine meadow taxa underline the shift from a relatively cold and wet climate to a rather warm and dry environment during the last 130 years.

Despite the consistency of the data, the tentative character of our interpretation should be acknowledged. In addition to the limited sample number, the soil/sediment profile provides a lower pollen count than typical peat and lake sediments. Moreover, the pollen assemblages in the soil/sediments profile may be biased towards pollen with decay-resistant walls due to unfavorable biological and physical-chemical soil processes (Xu et al. 2016; Zhang et al. 2016). Nevertheless, in situations with limited pollen archives, palynological information from soils can still be valuable, although they should be interpreted with caution (Zhang et al. 2016). In future analyses determination of pollen concentration values by adding a tracer like *Lycopodium* spores (Stockmarr 1971) might help identifying pollen deposition and preservation processes.

COMPARISON WITH REGIONAL PALAEOCLIMATE RECORDS

The analyses of pollen assemblages extracted from the soil/sediment profile located in the alpine belt of the southern Mongolian Altai Mountains have led to the generalized tentative conclusion of the existence of a warm and dry phase between 2596 and 2254 cal a BP. This phase was presumably followed by a cold and wet phase lasting until 131 cal a BP, and then followed by another warm and dry phase up to recent times (***Figure 7***). According to a recent comprehensive review on the Holocene climatic and environmental history in Western Mongolia (Klinge and Sauer 2019), a sequence of such changes in temperature and humidity was observed in the Altai only once. The pollen data of a core obtained from the Yushenkule Peat in the alpine zone

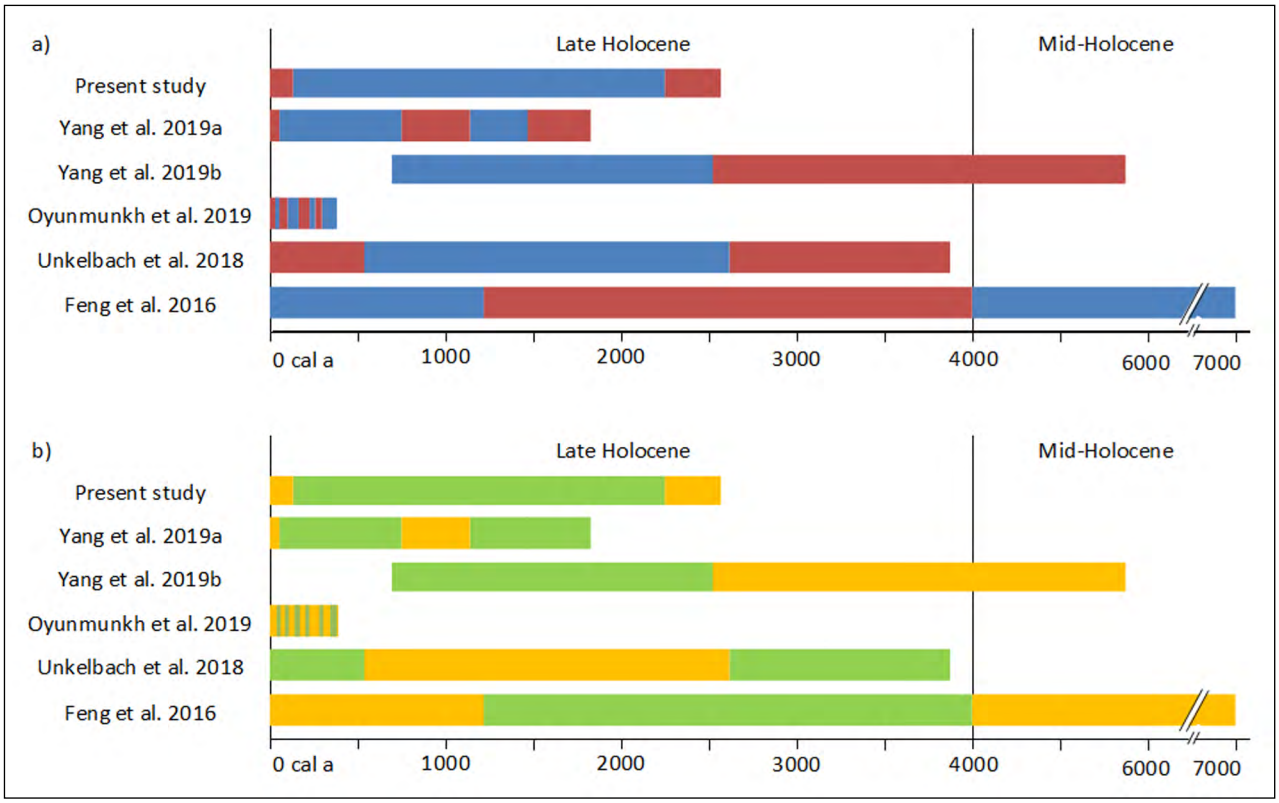

Figure 7 Synthesis of recent study results on periods of different temperature (a); warm = red, cold = blue) and moisture (b); green = wet, orange = dry) conditions in the southern Altai Mountains at the end of the Holocene.

of the Chinese southern Altai Mountains about 50 km from the present study site suggested a warm and dry period from 4870 to 2550 cal a BP, while a subsequent rather cold and wet environment was assumed until 700 cal a BP (Yang et al. 2019b). For the last 700 years, unfortunately no data were available. Based on the peat $\delta^{13}C_{celluose}$ signatures of the same core, a warm and wet period (Roman Warm Period from 1850 to 1450 a BP), a cool and wet phase (the Dark Age Cold Period from 1450 to 1150 a BP), a warm and dry interval (the Medieval Warm Period from 1150 to 750 a BP), a cool and wet period (the Little Ice Age from 750 to 50 a BP), and a warm and dry phase (Current Warm Period since 50 a BP) were proposed (Yang et al. 2019a). With the exception of the Roman Warm Period and the Medieval Warm Period, for which no results were obtained in the present study due to the absence of an organic layer or insufficient sample material in case of layer A5, the proposed tentative climatic conditions correspond very well to the presented observations in this study. For the period from 370 BP to 2012 CE, similarities in temperature and precipitation reconstructions are indicated by the comparison with tree ring analyses of *Larix sibirica* trees in the surroundings of the profile (Oyunmunkh et al. 2019). Likewise similar temperature and humidity conditions were deduced for both the Little Ice Age (cold and wet until 1874) and the 20th century (warm and dry), although a much more varied sequence of climate variation was observed (including cool/dry and warm/wet phases) due to the much higher temporal resolution. However, the comparison with high-resolution palynological analyses of a sediment core obtained from a peat bog formation in the south of Lake Dayan Nuur in the northern Mongolian Altai Mountains revealed similarities in the sequence and timing of changes in temperature but not in humidity. The data suggested a warm and wet climate from 3880 to 2610 cal BP and for the last 550 years, while cold and dry conditions were assumed for the interval in between (Unkelbach et al. 2018). Even less comparable is the climate variation inferred from the results of analyzed pollen data extracted from a core of the Narenxia Peat in the region of the Kanas Lake Basin in the Chinese Altai. Data suggested a cool and dry mid Holocene (7000 to 4000 a BP), a warm and wet Late Holocene (4000 to 1200 a BP) followed by a relatively cool and dry phase (past 1200 years) (Feng et al. 2017). The tentative results of the present study support not only the results reported for the nearby Yushenkule Peat core from the southern Chinese Altai, but also the observation of significant differences in the mode of climate variability and its temporal sequence even within the southern Altai Mountains. Nonetheless, it cannot be excluded that the non-analyses of B-layers for palynomorphs may have resulted in omission of temperature and moisture variations between the A-layers.

SEDIMENTOLOGICAL AND GEOCHEMICAL INDICATIONS

The sediment/soil profile was formed by sedimentation processes and *in situ* pedological forming processes overlying a well-developed palaeosol dated 5643 cal a BP (***Figure 3***). Phases of geomorphological instability are indicated by increased concentrations of P in B-layers compared to values in A-layers, pointing to sedimentation processes (Poudel et al. 1999; Ni and Zhang 2007; Lehmkuhl et al. 2011). Evidence for soil disturbances and erosive processes are additionally provided by the occurrence of Cichorioideae and Asteraceae pollen (Andreev et al. 2011) and spores of *Glomus* (Rudaya et al. 2008; Lehmkuhl et al. 2011) throughout the profile (***Figure 6***). During phases of geomorphological stability, humus accumulated leading to the thin A-layers with increased $C_{organic}$ and N_{total} concentrations. Due to the age determination using humic acids, mean values for the age of the fossil humus layers are given and no conclusions can thus be drawn about the duration of accumulation (Klinge and Sauer 2019) and the respective climate conditions. Short interruptions with more humid climatic conditions might have favored increased biomass production and humus accumulation. Extended phases of cool climatic conditions would have also increased the organic matter content due to a reduced biological decomposition of plant material (Klinge and Sauer 2019).

The content of coarse fragments in the layers and the sedimentation rate provide more information on the type of sedimentation processes. The lack of gravel and the low sedimentation rate suggest aeolian sedimentation for layer B9 favored by dry climate conditions, while the occurrence of non-rounded gravel indicates debris flow or solifluction for the B-layers 1 to 8 favoured by wet conditions and, in the case of solifluction, additionally by cold temperatures (Schlütz and Lehmkuhl 2007; Lehmkuhl 2016; Klinge and Sauer 2019). The climatic evidence for layers A2 to A6 (cold and wet) deduced from the palynological data support the aforementioned assumed geomorphological processes. For A10 no sound pollen data could be obtained. However, a warm and dry period was observed in the area of the Yushenkule peat for the period between 4870 and 2550 cal a BP, which can also be assumed for the present study area because of the strong similarities between the subsequent periods of the two investigated sites (Yang et al. 2019b). The supposed aeolian sedimentation process for layer B9 provides evidence for the assumption of a warm climate prevailing during this period. Only the layers B7 and B8 do not conform to the assumed climate conditions (warm and dry) as they contain coarse fragments, thus pointing to possible further causes of geomorphological instability such as fire and anthropozoogenic-influence. A fire event may lead to a partial or complete loss of vegetation cover having a negative effect on physical

soil properties such as infiltration rate, thus increasing the susceptibility of the soil towards erosive processes (Moody et al. 2013). This relationship can be observed not only in layer A9 but also in A7, A4 and A2. They all show abundance of micro-charcoal particles and are overlaid by a layer with a high sedimentation rate. For layers B6, B4, and B1 this is also attributable to solifluction due to the presumed cold and wet climate conditions. In layer A2, additionally, Ascomycetes spores are observed, which occur frequently in charred plant biomass and in dung (van Geel and Aptroot 2006). This supports together with the high abundance of *Glomus* sp. spores the assumption of local erosion processes caused by vegetation disturbances through fire events and animal trampling (Ejarque et al. 2010; López-Vila et al. 2014). The gravel-containing layer B7 was deposited during a transitional period from warm and dry to cold and wet climate conditions likely pointing to solifluction and/or anthropogenic-influence. The underlying layer A8 shows high percentages of Cichorioideae and Asteraceae as well as *Potentilla* and Caryophyllaceae in combination with *Artemisia*, indicating soil disturbances and erosive processes (Andreev et al. 2011) and moderate to heavy grazing activities (Li et al. 2008). Livestock-induced trampling and grazing at high stocking densities can lead to a decrease in topsoil stability (Taboada et al. 2011) followed by debris flow events after snowmelt or heavy rainfall, which could even be exacerbated by the already sparse vegetation cover under arid climate conditions. In summary, the geomorphological processes explaining the sedimentation rates and gravel content of the B-layers correspond to the assumed temperature and humidity conditions based on the pollen analyses and the findings of micro-charcoal particles. Only the formation of the sedimentation layer B7 is ambiguous and could be due to an anthropozoogenic influence and/or solifluction processes.

INDICATIONS OF ANTHROPO-ZOOGENIC INFLUENCE

The Altai Mountains were populated by humans since the Paleolithic (Shunkov 2005; Derevianko et al. 2013), whereby the anthropo-zoogenic impact on the environment increased significantly, latest with the arrival of Scythian pastoralists to the Altai Mountains by about 3000 a BP (Schlütz and Lehmkuhl 2007; Klinge and Sauer 2019). The current alpine vegetation in the surroundings of the studied site is seasonally grazed by livestock of transhumant pastoralists (Jordan et al. 2016). Since the pollen spectra of the analyzed layers of the profile provide evidence that the local alpine meadow/alpine steppe vegetation has remained rather stable over the last 2600 years, it can be assumed that this area has been used as summer pasture during the last few thousand years. In addition to several stone graves (kurgans) near the profile site, the characteristics of pollen assemblages throughout the profile support this assumption of an anthropo-zoogenic influence. Relatively high percentages of *Artemisia*, Asteraceae, Caryophyllaceae, Chenopodiaceae, Cichorioideae, Cyperaceae, *Iris* spec., *Potentilla*, and Rubiaceae (cf. *Galium*) throughout the profile, together with a high N input and disturbed soils, all suggest a moderate to high grazing intensity (Li et al. 2008; Baranova et al. 2016; Li et al. 2015; Andreev et al. 2011). Such a moderate to high grazing intensity can damage the soil structure and the susceptible alpine vegetation cover not only under dry climatic conditions as discussed previously, but can also accelerate debris flow or solifluction under wet conditions. Likewise, fire events negatively affect plants and soil and can result in increased sedimentation as already demonstrated, although human-induced fires as the cause of geomorphological instability cannot be substantiated from this study. Following the inhabitation of the Altai by Scythian pastoralists starting at about 3000 years ago, a strong decline of former forested areas was observed in the Altai (Blyakharchuk et al. 2007; Unkelbach et al. 2018). The likely existence of a forest prior the arrival of Scythian pastoralists in the study area may be reflected by the occurrence of bone fragments of musk deer that prefer forested habitats. But whether the high amount of microcharcoal particles in A9 is indeed linked to human-induced burning to improve pasture productivity or convert forested areas into pasture land, as it was likely common in this region (Unkelbach et al. 2018), remains questionable. Nevertheless, it is interesting to note that the geomorphological intensity increased from about 2600 a BP onwards, which does not coincide with the turning point of the climatic conditions, but rather with the assumed advent of pastoralism. Similar observations were made for four different geomorphological aeolian and fluvial archives across western Mongolia (Klinge et al. 2017). The impact of the anthropo-zoogenic activity on vegetation is of particular importance for the reconstruction of the palaeoclimate, as pollen assemblages may be biased and thus hampering interpretation (Li et al. 2014). A recent systematic review of literature in Mongolian language (Munkhzul et al. 2021) showed a negative impact of grazing on above-ground biomass and species richness in high mountain steppes of Mongolia while having no effects on vegetation cover. However, as shown by the good agreement with data from the Yushenkule Peat core, the climate signals of the vegetation do not seem to have been excessively affected by anthropogenic influence. It seems that, as has been shown for the alpine vegetation on the Tibetan Plateau (Ma et al. 2020), the climate was far more decisive concerning vegetation and floral composition than anthropogenic effects, so that regional climate signals can still be detected.

CONCLUSIONS

The analyses of pollen assemblages extracted from a soil/sediment profile located in the alpine belt of the southern Mongolian Altai Mountains led to the generalized assumption of a warm and dry phase between 2596 and 2254 cal a BP presumably followed by a cold and wet phase lasting until 131 cal a BP, and succeeded by the current warm and dry phase. Despite its relatively limited sample number and low pollen counts per sample the present study supports not only the results reported for the nearby Yushenkule Peat core from the southern Chinese Altai, but also the observation of significant differences in the mode of climate variability and its temporal sequence within the southern Altai Mountains. Although a continuous anthropo-zoogenic impact on the vegetation in the surroundings of the profile was reflected in the pollen assemblages over the past 2600 years, the climatic signals of the vegetation during this period were still sufficiently detectable. The study thus underlines the likely suitability of pollen data obtained from rather particular alpine sediments, despite the often discussed limitations of such terrestrial profiles. These conclusions are supported by sedimentological and geochemical characteristics of the investigated sediment layers.

DATA ACCESSIBILITY STATEMENTS

All data generated or analyzed during this study are included in this published article and its supplementary information file. The dataset on palynological analysis is available from the corresponding author on reasonable request.

ACKNOWLEDGEMENTS

The authors are indebted to Oyundari Chuluunkhuyag from the Department of Biology at the National University of Mongolia in Ulaanbaatar for information on recent vegetation (2015). We also would like to thank Sabine Hansen and Mario Tucci (Leuphana University of Lüneburg, Germany) for laboratory treatment and pollen data processing with the TILIA software. The authors' special thanks go to Prof. Dr. Norbert Benecke, Deutsches Archäologisches Institut, Berlin (Germany), for the identification of bone fragments and to Prof. Dr. Karsten Wesche, Senckenberg Museum of Natural History, Görlitz (Germany), for help with pollen interpretation. We also thank the anonymous reviewers providing helpful comments on earlier drafts of the manuscript. This study was conducted as part of the WATERCOPE project funded by the International Fund for Agricultural Development IFAD, Rome, Italy (I-R-1284).

COMPETING INTERESTS

The authors have no competing interests to declare.

AUTHOR CONTRIBUTIONS

All authors have reviewed and agreed to the entire content of the manuscript. The specific contribution of the authors was as follows: SGJ and AB were involved in conceptualization and sampling. BU supervised laboratory analyses. SGJ and BU contributed to data management, statistical analyses, data presentation, data interpretation and manuscript writing.

AUTHOR AFFILIATIONS

Sven Goenster-Jordan *orcid.org/0000-0001-8769-337X*
University of Kassel, DE

Brigitte Urban
Leuphana University of Lüneburg, DE

Andreas Buerkert *orcid.org/0000-0003-1329-1559*
University of Kassel, DE

REFERENCES

Agatova, AR, Nazarov, AN, Nepop, RK and **Rodnight, H**. 2012. Holocene glacier fluctuations and climate changes in the southeastern part of the Russian Altai (South Siberia) based on a radiocarbon chronology. *Quaternary Science Reviews,* 43: 74–93. DOI: *https://doi.org/10.1016/j.quascirev.2012.04.012*

Aizen, VB, Aizen, EM, Fujita, K, Nikitin, SA, Kreutz, KJ and **Takeuchi, LN.** 2005. Stable-isotope time series and precipitation origin from firn-core and snow samples, Altai glaciers, Siberia. *Journal of Glaciology*, 51: 637–654. DOI: *https://doi.org/10.3189/172756505781829034*

Aizen, VB, Aizen, EM, Joswiak, DR, Fujita, K, Takeuchi, N and **Nikitin, SA.** 2006. Climatic and atmospheric circulation pattern variability from ice-core isotope/geochemistry records (Altai, Tien Shan and Tibet). *Annals of Glaciology,* 43(1): 49–60. DOI: *https://doi.org/10.3189/172756406781812078*

Andreev, AA, Schirrmeister, L, Tarasov, PE, Ganopolski, A, Brovkin, V, Siegert, C, Wetterich, S and **Hubberten, H-W.** 2011. Vegetation and climate history in the Laptev Sea region (Arctic Siberia) during Late Quaternary inferred from pollen records. *Quaternary Science Reviews,* 30(17–18): 2182–2199. DOI: *https://doi.org/10.1016/j.quascirev.2010.12.026*

Bałaga, K and **Chodorowski, J.** 2006. Pollen analysis from fossil podzol soils within a dune at Kaczórki (Middle Roztocze, Poland). *Acta Palaeobotanica,* 46(2): 245–254.

Baranova, A, Schickhoff, U, Wang, S and **Jin, M.** 2016. Mountain pastures of Qilian Shan. Plant communities, grazing impact and degradation status (Gansu province, NW China). *Hacquetia,* 15(2): 21–35. DOI: *https://doi.org/10.1515/hacq-2016-0014*

Beug, HJ. 2004. *Leitfaden der Pollenbestimmung für Mitteleuropa und angrenzende Gebiete*. München, Germany: Verlag Dr. Friedrich Pfeil.

Bezuglova, NN, Zinchenko, GS, Malygina, NS, Papina, TS and **Barlyaeva, TV.** 2012. Response of high-mountain Altai thermal regime to climate global warming of recent decades. *Theoretical and Applied Climatology,* 110(4): 595–605. DOI: *https://doi.org/10.1007/s00704-012-0710-2*

Blume, H-P, Stahr, K and **Leinweber, P.** 2011. *Bodenkundliches Praktikum*. Heidelberg, Germany: Spektrum Akademischer Verlag. DOI: *https://doi.org/10.1007/978-3-8274-2733-5*

Blyakharchuk, TA, Wright, HE, Borodavko, PS, van der Knaap, WO and **Ammann, B.** 2007. Late Glacial and Holocene vegetational history of the Altai Mountains (southwestern Tuva Republic, Siberia). *Palaeogeography, Palaeoclimatology, Palaeoecology,* 245: 518–534. DOI: *https://doi.org/10.1016/j.palaeo.2006.09.010*

Blyakharchuk, TA, Wright, HE, Borodavko, PS, van der Knaap, WO and **Ammann, B.** 2008. The role of pingos in the development of the Dzhangyskol lake-pingo complex, central Altai Mountains, southern Siberia. *Palaeogeography, Palaeoclimatology, Palaeoecology,* 257(4): 404–420. DOI: *https://doi.org/10.1016/j.palaeo.2007.09.015*

Bray, RH and **Kurtz, LT.** 1945. Determination of total, organic and available forms of phosphorus in soils. *Soil Science,* 59: 39–45. DOI: *https://doi.org/10.1097/00010694-194501000-00006*

Brugger, SO, Gobet, E, Sigl, M, Osmont, D, Papina, T, Rudaya, N, Schwikowski, M and **Tinnera, W.** 2018. Ice records provide new insights into climatic vulnerability of Central Asian forest and steppe communities. *Global and Planetary Change*, 169: 188–201. DOI: *https://doi.org/10.1016/j.gloplacha.2018.07.010*

Buso Junior, AA, Pessenda, LCR, Mayle, FE, Lorente, FL, Volkmer-Ribeiro, C, Schiavo, JA, Pereira, MG, Bendassolli, JA, Macario, KCD and **Siqueira, GS.** 2019. Paleovegetation and paleoclimate dynamics during the last 7000 years in the Atlantic forest of Southeastern Brazil based on palynology of a waterlogged sandy soil. *Review of Palaeobotany and Palynology,* 264: 1–10. DOI: *https://doi.org/10.1016/j.revpalbo.2019.02.002*

Chen, F, Yu, Z, Yang, M, Ito, E, Wang, S, Madsen, DB, Huang, X, Zhao, Y, Sato, T, John B. Birks, H, Boomer, I, Chen, J, An, C and **Wünnemann, B.** 2008. Holocene moisture evolution in arid central Asia and its out-of-phase relationship with Asian monsoon history. *Quaternary Science Reviews,* 27(3): 351–364. DOI: *https://doi.org/10.1016/j.quascirev.2007.10.017*

Davidson, DA, Carter, S, Boag, B, Long, D, Tipping, R and **Tyler, A.** 1999. Analysis of pollen in soils. processes of incorporation and redistribution of pollen in five soil profile types. *Soil Biology and Biochemistry,* 31(5): 643–653. DOI: *https://doi.org/10.1016/S0038-0717(98)00123-0*

Derevianko, AP, Markin, SV, Zykin, VS, Zykina, VS, Zazhigin, VS, Sizikova, AO, Solotchina, EP, Smolyaninova, LG and **Antipov, AS.** 2013. Chagyrskaya Cave. A Middle Paleolithic site in the Altai. *Archaeology, Ethnology and Anthropology of Eurasia,* 41(1): 2–27. DOI: *https://doi.org/10.1016/j.aeae.2013.07.002*

Dimbleby, GW. 1952. The historical status of moorland in north-east Yorkshire. *New Phytologist,* 51(3): 349–354. DOI: *https://doi.org/10.1111/j.1469-8137.1952.tb06142.x*

Dulamsuren, C, Khishigjargal, M, Leuschner, C and **Hauck, M.** 2014. Response of tree-ring width to climate warming and selective logging in larch forests of the Mongolian Altai. *Journal of Plant Ecology,* 7(1): 24–38. DOI: *https://doi.org/10.1093/jpe/rtt019*

Ejarque, A, Miras, Y, Riera, S, Palet, JM and **Orengo, HA.** 2010. Testing micro-regional variability in the Holocene shaping of high mountain cultural landscapes. A palaeoenvironmental case-study in the eastern Pyrenees. *Journal of Archaeological Science,* 37(7): 1468–1479. DOI: *https://doi.org/10.1016/j.jas.2010.01.007*

Fægri, K, Kaland, PE and **Krzywinski, K.** 1989. *Textbook of pollen analysis*. Chichester, United Kingdom: John Wiley & Sons Ltd.

Fedeneva, IN and **Dergacheva, MI.** 2003. Paleosols as the basis of environmental reconstruction in Altai mountainous areas. *Quaternary International,* 106–107: 89–101. DOI: *https://doi.org/10.1016/S1040-6182(02)00164-7*

Feng, Z, Sun, A, Abdusalih, N, Ran, M, Kurban, A, Lan, B, Zhang, D and **Yang, Y.** 2017. Vegetation changes and associated climatic changes in the southern Altai Mountains within China during the Holocene. *The Holocene*, 27(5): 683–693. DOI: *https://doi.org/10.1177/0959683616670469*

Ganyushkin, D, Chistyakov, K, Volkov, I, Bantcev, D, Kunaeva, E, Brandová, D, Raab, G, Christl, M and **Egli, M.** 2018. Palaeoclimate, glacier and treeline reconstruction based on geomorphic evidences in the Mongun-Taiga massif (south-eastern Russian Altai) during the Late Pleistocene and Holocene. *Quaternary International,* 470: 26–37. DOI: *https://doi.org/10.1016/j.quaint.2017.12.031*

Grimm, EC. 1990. TILIA and TILIA. GRAPH. PC spreadsheet and graphics software for pollen data (Version 2.0.b.4). INQUA – Commission for the Study of the Holocene, Working-Group on Data-Handling Methods. *Newsletter,* 4: 5–7.

Grunert, J, Lehmkuhl, F and **Walther, M.** 2000. Paleoclimatic evolution of the Uvs Nuur basin and adjacent areas (Western Mongolia). *Quaternary International,* 65–66: 171–192. DOI: *https://doi.org/10.1016/S1040-6182(99)00043-9*

Gunin, PD, Vostokova, EA, Dorofeyuk, NI, Tarasov, PE and **Black, CC.** 1999. *Vegetation dynamics of Mongolia*. Dordrecht, The Netherlands, Boston, London, United Kingdom: Kluwer Academic Publishers. DOI: *https://doi.org/10.1007/978-94-015-9143-0*

Herren, P-A. 2013. *Ice core based climate reconstruction from the Mongolian Altai.* Unpublished thesis (PhD), University of Bern.

Herzschuh, U. 2007. Reliability of pollen ratios for environmental reconstructions on the Tibetan Plateau. *Journal of Biogeography,* 34(7): 1265–1273. DOI: *https://doi.org/10.1111/j.1365-2699.2006.01680.x*

Herzschuh, U, Tarasov, P, Wünnemann, B and **Hartmann, K.** 2004. Holocene vegetation and climate of the Alashan Plateau, NW China, reconstructed from pollen data. *Palaeogeography, Palaeoclimatology, Palaeoecology,* 211(1–2): 1–17. DOI: *https://doi.org/10.1016/j.palaeo.2004.04.001*

Herzschuh, U, Winter, K, Wünnemann, B and **Li, S.** 2006. A general cooling trend on the central Tibetan Plateau throughout the Holocene recorded by the Lake Zigetang pollen spectra. *Quaternary International,* 154–155: 113–121. DOI: *https://doi.org/10.1016/j.quaint.2006.02.005*

Hilbig, W. 1995. *The vegetation of Mongolia.* Amsterdam, The Netherlands: SPB Academic Publishing.

Huang, X, Peng, W, Rudaya, N, Grimm, EC, Chen, X, Cao, X, Zhang, J, Pan, X, Liu, S, Chen, C and **Chen, F.** 2018. Holocene vegetation and climate dynamics in the Altai Mountains and surrounding areas. *Geophysical Research Letters,* 45(13): 6628–6636. DOI: *https://doi.org/10.1029/2018GL078028*

Jordan, G, Goenster, S, Munkhnasan, T, Shabier, A, Buerkert, A and **Schlecht, E.** 2016. Spatio-temporal patterns of herbage availability and livestock movements: A cross-border analysis in the Chinese-Mongolian Altay. *Pastoralism: Research, Policy and Practice,* 6: 1–17. DOI: *https://doi.org/10.1186/s13570-016-0060-2*

Kalugin, I, Selegei, V, Goldberg, E and **Seret, G.** 2005. Rhythmic fine-grained sediment deposition in Lake Teletskoye, Altai, Siberia, in relation to regional climate change. *Quaternary International*, 136(1): 5–13. DOI: *https://doi.org/10.1016/j.quaint.2004.11.003*

Klinge, M, Böhner, J and **Lehmkuhl, F.** 2003. Climate pattern, snow- and timberlines in the Altai Mountains, Central Asia. *Erdkunde,* 57(4): 296–307. DOI: *https://doi.org/10.3112/erdkunde.2003.04.04*

Klinge, M, Lehmkuhl, F, Schulte, P, Hülle, D and **Nottebaum, V.** 2017. Implications of (reworked) aeolian sediments and paleosols for Holocene environmental change in Western Mongolia. *Geomorphology,* 292: 59–71. DOI: *https://doi.org/10.1016/j.geomorph.2017.04.027*

Klinge, M and **Sauer, D.** 2019. Spatial pattern of Late Glacial and Holocene climatic and environmental development in Western Mongolia – A critical review and synthesis. *Quaternary Science Reviews,* 210: 26–50. DOI: *https://doi.org/10.1016/j.quascirev.2019.02.020*

Kürschner, H, Herzschuh, U and **Wagner, D.** 2005. Phytosociological studies in the north-eastern Tibetan Plateau (NW China) A first contribution to the subalpine scrub and alpine meadow vegetation. *Botanische Jahrbücher für Systematik, Pflanzengeschichte und Pflanzengeographie,* 126(3): 273–315. DOI: *https://doi.org/10.1127/0006-8152/2005/0126-0273*

Lang, G. 1994. *Quartäre Vegetationsgeschichte Europas – Methoden und Ergebnisse*. Stuttgart, Jena, Germany: Gustav Fischer Verlag.

Lehmkuhl, F. 2016. Modern and past periglacial features in Central Asia and their implication for paleoclimate reconstructions. *Progress in Physical Geography,* 40(3): 369–391. DOI: *https://doi.org/10.1177/0309133315615778*

Lehmkuhl, F, Hilgers, A, Fries, S, Hülle, D, Schlütz, F, Shumilovskikh, L, Felauer, T and **Protze, J.** 2011. Holocene geomorphological processes and soil development as indicator for environmental change around Karakorum, Upper Orkhon Valley (Central Mongolia). *Catena,* 87(1): 31–44. DOI: *https://doi.org/10.1016/j.catena.2011.05.005*

Li, F, Sun, J, Zhao, Y, Guo, X, Zhao, W and **Zhang, K.** 2010. Ecological significance of common pollen ratios. A review. *Frontiers of Earth Science in China,* 4(3): 253–258. DOI: *https://doi.org/10.1007/s11707-010-0112-7*

Li, J, Zhao, Y, Xu, Q, Zheng, Z, Lu, H, Luo, Y, Li, Y, Li, C and **Seppä, H.** 2014. Human influence as a potential source of bias in pollen-based quantitative climate reconstructions. *Quaternary Science Reviews*, 99: 112–121. DOI: *https://doi.org/10.1016/j.quascirev.2014.06.005*

Li, M, Xu, Q, Zhang, S, Li, Y, Ding, W and **Li, J.** 2015. Indicator pollen taxa of human-induced and natural vegetation in Northern China. *The Holocene,* 25(4): 686–701. DOI: *https://doi.org/10.1177/0959683614566219*

Li, Y, Zhou, L and **Cui, H.** 2008. Pollen indicators of human activity. *Chinese Science Bulletin,* 53(9): 1281–1293. DOI: *https://doi.org/10.1007/s11434-008-0181-0*

López-Vila, J, Montoya, E, Cañellas-Boltà, N and **Rull, V.** 2014. Modern non-pollen palynomorphs sedimentation along an elevational gradient in the south-central Pyrenees (southwestern Europe) as a tool for Holocene paleoecological reconstruction. *The Holocene,* 24(3): 327–345. DOI: *https://doi.org/10.1177/0959683613518593*

Ma, Q, Zhu, L, Wang, J, Ju, J, Wang, Y, Lü, X, Kasper, T and **Haberzettl, T.** 2020. Late Holocene vegetation responses to climate change and human impact on the central Tibetan Plateau. *Science of the Total Environment,* 708: 135370. DOI: *https://doi.org/10.1016/j.scitotenv.2019.135370*

Moody, JA, Shakesby, RA, Robichaud, PR, Cannon, SH and **Martin, DA.** 2013. Current research issues related to post-wildfire runoff and erosion processes. *Earth-Science Reviews*, 122: 10–37. DOI: *https://doi.org/10.1016/j.earscirev.2013.03.004*

Moore, PD, Webb, JA and **Collison, ME.** 1991. *Pollen analysis*. Oxford, United Kingdom: Blackwell Scientific Publications.

Munkhzul, O, Oyundelge, K, Narantuya, N, Tuvshintogtokh, I, Oyuntsetseg, B, Wesche, K and **Jäschke, Y.** 2021. Grazing Effects on Mongolian Steppe Vegetation — A Systematic Review of Local Literature. *Frontiers in Ecology and Evolution*, 9: 703220. DOI: *https://doi.org/10.3389/fevo.2021.703220*

Myglan, VS, Oidupaa, OC and **Vaganov, EA.** 2012. A 2367-year tree-ring chronology for the Altai-Sayan Region (Mongun-Taiga Mountain Massif). *Archaeology, Ethnology and Anthropology of Eurasia,* 40(3): 76–83. DOI: *https://doi.org/10.1016/j.aeae.2012.11.009*

Ni, SJ and **Zhang, JH.** 2007. Variation of chemical properties as affected by soil erosion on hillslopes and terraces. *European Journal of Soil Science,* 58(6): 1285–1292. DOI: *https://doi.org/10.1111/j.1365-2389.2007.00921.x*

Oyunmunkh, B, Weijers, S, Loeffler, J, Byambagerel, S, Soninkhishig, N, Buerkert, A, Goenster-Jordan, S and **Simmer, C.** 2019. Climate variations over the southern Altai Mountains and Dzungarian Basin region, central Asia, since 1580 CE. *International Journal of Climatology,* 39(11): 4543–4558. DOI: *https://doi.org/10.1002/joc.6097*

Poudel, DD, Midmore, DJ and **West, LT.** 1999. Erosion and productivity of vegetable systems on sloping volcanic ash-derived Philippine soils. *Soil Science Society of America Journal,* 63(5): 1366–1376. DOI: *https://doi.org/10.2136/sssaj1999.6351366x*

Reimer, PJ, Austin, WEN, Bard, E, Bayliss, A, Blackwell, PG, Bronk Ramsey, C, Butzin, M, Cheng, H, Edwards, RL, Friedrich, M, Grootes, PM, Guilderson, TP, Hajdas, I, Heaton, TJ, Hogg, AG, Hughen, KA, Kromer, B, Manning, SW, Muscheler, R, Palmer, JG, Pearson, C, van der Plicht, J, Reimer, RW, Richards, DA, Scott, EM, Southon, JR, Turney, CSM, Wacker, L, Adolphi, F, Büntgen, U, Capano, M, Fahrni, SM, Fogtmann-Schulz, A, Friedrich, R, Köhler, P, Kudsk, S, Miyake, F, Olsen, J, Reinig, F, Sakamoto, M, Sookdeo, A and **Talamo, S.** 2020. The IntCal20 Northern Hemisphere Radiocarbon Age Calibration Curve (0–55 cal kBP). *Radiocarbon*, 62(4): 725–757. DOI: *https://doi.org/10.1017/RDC.2020.41*

Rudaya, N and **Li, H-C.** 2013. A new approach for reconstruction of the Holocene climate in the Mongolian Altai. The high-resolution δC records of TOC and pollen complexes in Hoton-Nur Lake sediments. *Journal of Asian Earth Sciences,* 69: 185–195. DOI: *https://doi.org/10.1016/j.jseaes.2012.12.002*

Rudaya, N, Tarasov, P, Dorofeyuk, N, Solovieva, N, Kalugin, I, Andreev, A, Daryin, A, Diekmann, B, Riedel, F, Tserendash, N and **Wagner, M.** 2009. Holocene environments and climate in the Mongolian Altai reconstructed from the Hoton-Nur pollen and diatom records. a step towards better understanding climate dynamics in Central Asia. *Quaternary Science Reviews,* 28 (5–6): 540–554. DOI: *https://doi.org/10.1016/j.quascirev.2008.10.013*

Rudaya, NA, Tarasov, PE, Dorofeyuk, NI, Kalugin, IA, Andreev, AA, Diekmann, B and **Daryin, AV.** 2008. Environmental changes in the Mongolian Altai during the Holocene. *Archaeology Ethnology & Anthropology of Eurasia,* 36(4): 2–14. DOI: *https://doi.org/10.1016/j.aeae.2009.03.001*

Schlütz, F and **Lehmkuhl, F.** 2007. Climatic change in the Russian Altai, southern Siberia, based on palynological and geomorphological results, with implications for climatic teleconnections and human history since the middle Holocene. *Vegetation History and Archaeobotany,* 16(2–3): 101–118. DOI: *https://doi.org/10.1007/s00334-006-0073-7*

Schwikowski, M, Eichler, A, Kalugin, I, Ovtchinnikov, D and **Papina, T.** 2009. Past climate variability in the Altai. *PAGES News,* 17(1): 44–45. DOI: *https://doi.org/10.22498/pages.17.1.44*

Shunkov, M. 2005. The characteristics of the Altai (Russia) Middle Paleolithic in regional context. *Bulletin of the Indo-Pacific Prehistory Association,* 25, The Taipei Papers (3): 69–77.

Stockmarr, J. 1971. Tablets with Spores used in Absolute Pollen Analysis. *Pollen et Spores*, 13: 614–621.

Sun, C, Li, J and **Zhao, S.** 2015. Remote influence of Atlantic multidecadal variability on Siberian warm season precipitation. *Scientific Reports,* 5: 16853. DOI: *https://doi.org/10.1038/srep16853*

Taboada, MA, Rubio, G, Chaneton, EJ, Hatfield, JL and **Sauer, TJ.** 2011. Grazing impacts on soil physical, chemical, and ecological properties in forage production systems. In Hatfield, JL and Sauer, TJ (eds.), *Soil management. Building a stable base for agriculture*, 301–320. Madison, Wisconsin, USA: American Society of Agronomy, Soil Science Society of America. DOI: *https://doi.org/10.2136/2011.soilmanagement.c20*

Tarasov, P, Dorofeyuk, N and **Metel'Tseva, E**. 2000. Holocene vegetation and climate changes in Hoton-Nur basin, northwest Mongolia. *Boreas*, 29(2): 117–126. DOI: *https://doi.org/10.1111/j.1502-3885.2000.tb01205.x*

Tarasov, PE, Cheddadi, R, Guiot, J, Bottema, S, Peyron, O, Belmonte, J, Ruiz-Sanchez, V, Saadi, F and **Brewer, S.** 1998. A method to determine warm and cool steppe biomes from pollen data; application to the Mediterranean and Kazakhstan regions. *Journal of Quaternary Science,* 13(4): 335–344. DOI: *https://doi.org/10.1002/(SICI)1099-1417(199807/08)13:4<335::AID-JQS375>3.0.CO;2-A*

Targulian, VO, Arnold, RW, Miller, BA and **Brevik, EC.** 2019. Pedosphere. In Fath, B (ed.). *Encyclopedia of ecology*, 162–168. Oxford, United Kingdom: Elsevier. DOI: *https://doi.org/10.1016/B978-0-12-409548-9.11153-4*

Tian, F, Herzschuh, U, Telford, RJ, Mischke, S, van der Meeren, T and **Krengel, M.** 2014. A modern pollen–climate calibration set from central-western Mongolia and its application to a late glacial–Holocene record. *Journal of Biogeography*, 41(10): 1909–1922. DOI: *https://doi.org/10.1111/jbi.12338*

Unkelbach, J, Dulamsuren, C, Punsalpaamuu, G, Saindovdon, D and **Behling, H.** 2018. Late Holocene vegetation, climate, human and fire history of the forest-steppe-ecosystem inferred from core G2-A in the 'Altai Tavan Bogd' conservation area in Mongolia. *Vegetation History and Archaeobotany,* 27(5): 665–677. DOI: *https://doi.org/10.1007/s00334-017-0664-5*

van Geel, B and **Aptroot, A.** 2006. Fossil ascomycetes in Quaternary deposits. *Nova Hedwigia,* 82(3): 313–329. DOI: *https://doi.org/10.1127/0029-5035/2006/0082-0313*

Wang, W and **Feng, Z.** 2013. Holocene moisture evolution across the Mongolian Plateau and its surrounding areas. A synthesis of climatic records. *Earth-Science Reviews*, 122: 38–57. DOI: *https://doi.org/10.1016/j.earscirev.2013.03.005*

Welten, M. 1957. Über das glaziale und spätglaziale Vorkommen von Ephedra am nordwestlichen Alpenrand. *Berichte der schweizerischen botanischen Gesellschaft*, 67: 33–54.

Westover, KS, Fritz, SC, Blyakharchuk, TA and **Wright, HE.** 2006. Diatom paleolimnological record of Holocene climatic and environmental change in the Altai Mountains, Siberia. *Journal of Paleolimnology,* 35: 519–541. DOI: *https://doi.org/10.1007/s10933-005-3241-3*

Xu, Q, Li, Y, Yang, X and **Zheng, Z.** 2007. Quantitative relationship between pollen and vegetation in northern China. *Science in China Series D: Earth Sciences,* 50(4): 582–599. DOI: *https://doi.org/10.1007/s11430-007-2044-y*

Xu, Q, Zhang, S, Gaillard, M-j, Li, M, Cao, X, Tian, F and **Li, F.** 2016. Studies of modern pollen assemblages for pollen dispersal- deposition- preservation process understanding and for pollen-based reconstructions of past vegetation, climate, and human impact. A review based on case studies in China. *Quaternary Science Reviews,* 149: 151–166. DOI: *https://doi.org/10.1016/j.quascirev.2016.07.017*

Yang, Y, Zhang, D, Lan, B, Abdusalih, N and **Feng, Z.** 2019a. Peat $\delta^{13}C_{cellulose}$-signified moisture variations over the past ∂200 years in the southern Altai Mountains, northwestern China. *Journal of Asian Earth Sciences,* 174: 59–67. DOI: *https://doi.org/10.1016/j.jseaes.2018.11.019*

Yang, Y, Zhang, D, Sun, A, Wang, W, Lan, B and **Feng, Z.** 2019b. Pollen-based reconstructions of vegetation and climate changes during the late Holocene in the southern Altai Mountains. *The Holocene,* 29(9): 1450–1458. DOI: *https://doi.org/10.1177/0959683619854515*

Yu, G, Prentice, IC, Harrison, SP and **Sun, X.** 2008. Pollen-based biome reconstructions for China at 0 and 6000 years. *Journal of Biogeography,* 25(6): 1055–1069. DOI: *https://doi.org/10.1046/j.1365-2699.1998.00237.x*

Zemmrich, A. 2008. The northern part of Khovd Province – An ecological introduction. *Hamburger Beiträge zur Physischen Geographie und Landschaftsökologie,* 18: 1–10.

Zemmrich, A, Manthey, M, Zerbe, S and **Oyunchimeg, D.** 2010. Driving environmental factors and the role of grazing in grassland communities. A comparative study along an altitudinal gradient in Western Mongolia. *Journal of Arid Environments,* 74(10): 1271–1280. DOI: *https://doi.org/10.1016/j.jaridenv.2010.05.014*

Zhang, D and **Feng, Z.** 2018. Holocene climate variations in the Altai Mountains and the surrounding areas. A synthesis of pollen records. *Earth-Science Reviews*, 185: 847–869. DOI: *https://doi.org/10.1016/j.earscirev.2018.08.007*

Zhang, D, Yang, Y and **Lan, B.** 2018. Climate variability in the northern and southern Altai Mountains during the past 50 years. *Scientific Reports*, 8(1): 3238. DOI: *https://doi.org/10.1038/s41598-018-21637-x*

Zhang, S, Xu, Q, Gaillard, MJ, Cao, X, Li, J, Zhang, L, Li, Y, Tian, F, Zhou, L, Lin, F and **Yang, X.** 2016. Characteristic pollen source area and vertical pollen dispersal and deposition in a mixed coniferous and deciduous broad-leaved woodland in the Changbai mountains, northeast China. *Vegetation History and Archaeobotany,* 25: 29–43. DOI: *https://doi.org/10.1007/s00334-015-0532-0*

Zhao, Y and **Herzschuh, U.** 2009. Modern pollen representation of source vegetation in the Qaidam Basin and surrounding mountains, north-eastern Tibetan Plateau. *Vegetation History and Archaeobotany,* 18(3): 245–260. DOI: *https://doi.org/10.1007/s00334-008-0201-7*

TO CITE THIS ARTICLE:
Goenster-Jordan, S, Urban, B and Buerkert, A. 2022. Palaeoecological Interpretation of a Late Holocene Sediment Sequence from the Alpine Belt of the Southern Mongolian Altai Mountains. *Open Quaternary,* 8: 2, pp.1–18. DOI: *https://doi.org/10.5334/oq.90*

Submitted: 12 August 2020 Accepted: 01 February 2022 Published: 17 February 2022